

Supporting Information

For

Formation of linear supramolecular polymers that is based on host-guest assembly in water solution

Yongqian Xu,^a Mingming Guo^b, Xiaopeng Li^a, Andrey Malkovskiy^b, Chrys
Wesdemiotis^a and Yi Pang^{*a}

Department of Chemistry & Maurice Morton Institute of Polymer Science,
Department of Polymer Science, The University of Akron, Akron, OH, 44325

yp5@uakron.edu

1. Materials and general procedure

Thiazole Orange (TO) was purchased from Sigma-Aldrich and used without further purification. 1-amantadine hydrochloride (AD) was ordered from Acros. All the solvents and reagents were of analytic grade and used as received. Water used was ultra filter deionized and purchased from Fisher Scientific. NMR spectra were collected on Varian 300 and 500 Gemini spectrometers. Mass spectrometric data were obtained on a HP1100LC/MSD mass spectrometry. UV-Vis spectra were acquired on a Hewlett-Packard 8453 diode-array spectrometer. Fluorescence spectra were obtained on a HORIBA Jobin Yvon NanoLog spectrometer. CBs were synthesized as reported previously.^{S1} Dynamic light scattering (DLS) data was obtained on a Malvern Zetasizer Nano S (U.K., ZEN 3600) at 25 °C. AFM images were recorded under ambient conditions using a Park Scientific Autoprobe CP, which is operating in the tapping mode with Micromasch tapping probes with radius of curvature being <4 nm. The tips were brand new. Viscosity measurements were obtained from Haake Rotovisco 1 instrument at 25 °C.

S1. J. Kim, I. S. Jung, S. Y. Kim, E. Lee, J. K. Kang, S. Sakamoto, K. Yamaguchi, K. Kim, *J. Am. Chem. Soc.*, 2000, 122, 540-541.

2. NMR experiment.

All NMR samples were dissolving in D₂O and charge to 5 mm NMR tubes. All NMR experiments were recorded on a Varian VNMS 500 spectrometer at 25°C which equipped with a 10A z-axis gradient amplifier. ¹H chemical shifts were referenced to the HDO signal at δ 4.85 ppm. The proton 90° pulse width is 11 μs. The ¹H 2D ROESY spectra were acquired using the modified pulse sequence by Hwang and Shaka^{S2} with minimum TOCSY type artifact. The spin lock field used is 3600 Hz

during the mix time. Three mixing times, 200, 400 and 500 ms were used to acquire the 2D NMR data set using the states phase cycling. The presaturation was used right before the data acquisition to eliminate the huge water peak. The ^1H 2D DOSY spectra were acquired using the standard Varian pulse program, Dbppste, employing a double stimulated echo sequence, bipolar gradient pulses for diffusion, and three spoil gradients. The maxima PFG strength is 74 Gauss/cm based on the calibration results using doped D_2O sample and Varian profile sequence. To collect the DOSY data set, 15 different gradient levels were used during the fixed diffusion gradient length, δ , of 2 ms. The diffusion delay time, Δ , used is 50 ms. Individual rows of the quasi-2D diffusion databases were phased and baseline corrected.

Nuclear Overhauser effects are of paramount importance for conformational analysis in solution. Multidimensional methods such as NOESY are usually adequate for the highly inclusion complex spin systems. Application of traditional NOE difference methods is limited by the unfavorable tumbling rates τ_c of the compounds with molecular masses around 1000-2000 Da. The critical cross relaxation rate depends on the product of τ_c and the spectrometer frequency. In consequence, the conventional steady-state NOE is positive only for molecular masses well below 1000, and sizable negatives only for those well above 5000 Da.^{S3}

S2. Hwang, T. L.; Shaka, A. J. Cross Relaxation Without Tocsy-Transverse Rotating-Frame Overhauser Effect Spectroscopy. *J. Am. Chem. Soc.* **1992**, *114*, 3157-3159.

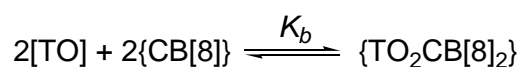
S3. Wu, D. H.; Chen, A. D.; Johnson, C. S. An Improved Diffusion-Ordered Spectroscopy Experiment Incorporating Bipolar-Gradient Pulses. *J. Magn. Reson. Ser. A* **1995**, *115*, 260-264

3. UV and fluorescence experiments

Stock solution (5.0×10^{-4} M) of **TO** in ethanol, stock solutions (5.0×10^{-4} M) of CBs in water were prepared. An aliquot (30 μL) of the **TO** stock solution was added to 3 mL water in a quartz cuvette. The sample was gently stirred for 5 s before the UV and fluorescence was recorded.

4. Determination of binding constant.

From the Job plot binding presented, the binding constant values for 1:2 and 2:2 stoichiometries with CB[7] and CB[8] respectively were evaluated by considering the following complexation equilibria



$$K_a = \{\text{TOCB}[7]_2\}/[\text{TO}]\{\text{CB}[7]\}^2 \quad (1)$$

$$K_b = \{\text{TO}_2\text{CB}[8]_2\}/[\text{TO}]^2\{\text{CB}[8]\}^2 \quad (2)$$

where K_a and K_b are the binding constants for the formation of the respective 1:2 and 2:2 complexes with CB[7] and CB[8] respectively.

For K_a , the binding constant value has been determined from the emission intensity data following the equation^{S4, S5}

$$Y = Y_0 + \frac{Y_{\text{lim}} - Y_0}{2} \left\{ 1 + \frac{C_M}{C_L} + \frac{1}{K_a C_L} - \left[\left(1 + \frac{C_M}{C_L} + \frac{1}{K_a C_L} \right)^2 - 4 \frac{C_M}{C_L} \right]^{1/2} \right\} \quad (3)$$

Y , Y_0 , and Y_{lim} are the recorded fluorescence intensity, fluorescence intensity without the addition of CB[7], and fluorescence at the limiting value, respectively, where C_M is the target molecule CB[7] concentration, C_L is the TO concentration, and K_a is the association constant. The following equation was used for the nonlinear least squares analysis to determine the association constant K_a .

For K_b , a simplified model reported in literature^{S6} was used to calculate the binding constant.

The conversion ratio of [TO] to $\{\text{TO}_2\text{CB}[8]_2\}$ [$\alpha = (I - I_0)/(I_\infty - I_0)$] is expressed by Equation (4),

$$\alpha = 2\{\text{TO}_2\text{CB}[8]_2\}/[\text{TO}]_0 \quad (4)$$

$$[\text{TO}]_0 = [\text{TO}] + 2\{\text{TO}_2\text{CB}[8]_2\} \quad (5)$$

where $[\text{TO}]_0$ is the total concentrations of TO used. I_0 and I_∞ are emission intensities without the addition of CB[8], and fluorescence at the maximum value, respectively, thus, Equation (6) is derived from Equation (2) and Equation (4)(5).

$$2K_b\{\text{CB}[8]\}^2[\text{TO}]_0 = \alpha/(1-\alpha)^2 \quad (6)$$

S4. Valeur, B. *Molecular Fluorescence: Principles and Applications*; Wiley-VCH: Weinheim, Germany, **2002**.

S5. Dhara, K.; Saha, U. C.; Dan, A.; Sarkar, S.; Manassero, M.; Chattopadhyay, P. *Chem. Commun.* **2010**, *46*, 1754.

S6. T. Ogawa, J. Yuasa, T. Kawai, *Angew. Chem. Int. Ed.* **2010**, *49*, 5110–5114.

5. Traveling wave ion mobility mass spectrometry (TWIM-MS) experiments

Traveling wave ion mobility mass spectrometry (TWIM-MS) experiments were performed using a Waters Synapt HDMS quadrupole/time-of-flight (Q/ToF) tandem mass spectrometer. The TWIM device is located between the Q and ToF mass

analyzers and consists of three parts, a trap cell, an ion mobility (IM) cell, and a transfer cell. The trap and transfer cells can be used for conventional tandem mass spectrometry experiments via collisionally activated dissociation (CAD). The ion mobility cell is used in IM separations. Generally, the following parameters were used in TWIM-MS experiments: ESI capillary voltage, 2.5 kV; sample cone voltage, 35 V; extraction cone voltage, 3.2 V; desolvation gas flow, 800 L/h (N₂); trap collision energy (CE), 6 eV; transfer CE, 4 eV; trap gas flow, 1.5 mL/min (Ar); IM gas flow, 22.7 mL/min (N₂); sample flow rate, 10 μL/min; source temperature, 30⁰C; desolvation temperature, 40⁰C; IM traveling wave velocity, 380 m/s. The sprayed solution was prepared by dissolving ~1 mg of sample in 1 mL of 3:1 H₂O/methanol solvent.

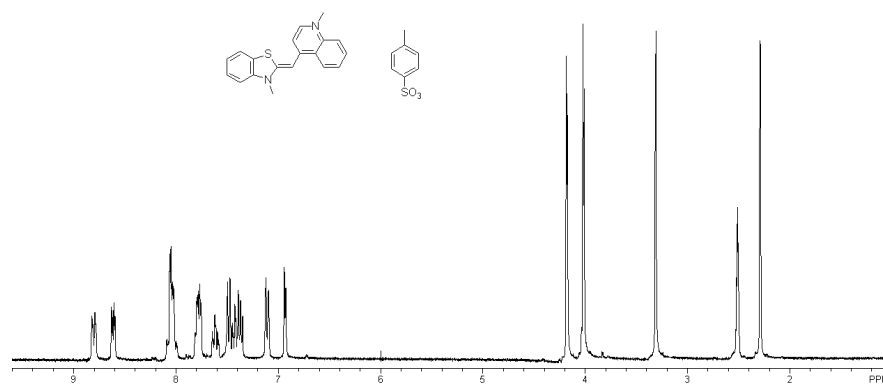
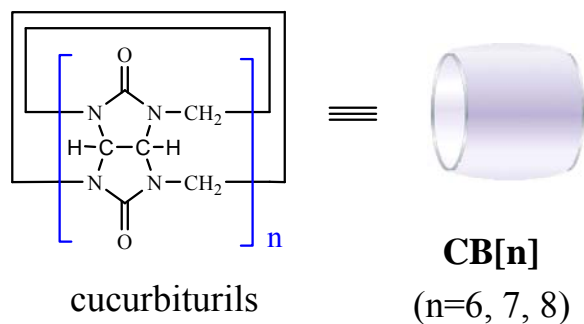


Fig S1. ¹H NMR spectrum of TO in DMSO-*d*₆.



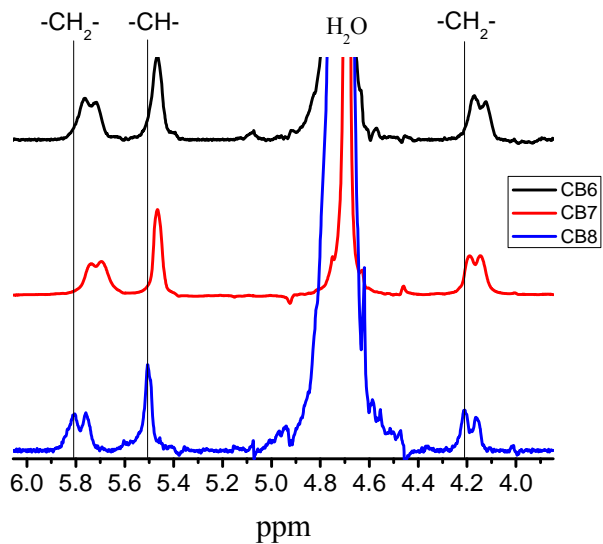
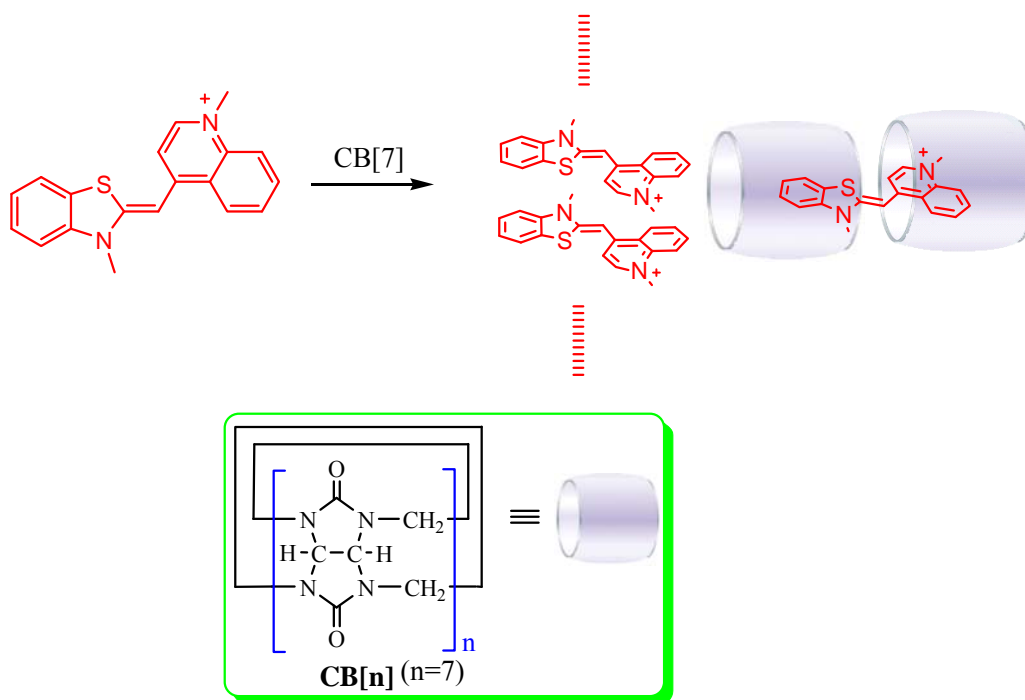


Fig S2. ¹H NMR spectrum of CBs (n=6-8) in D₂O.



Scheme S1. Structure of TO and schematic illustration of the TO-CB[7] assembly. In the structure of TO, the counter ion *p*-toluenesulfonate is not shown for clarity.

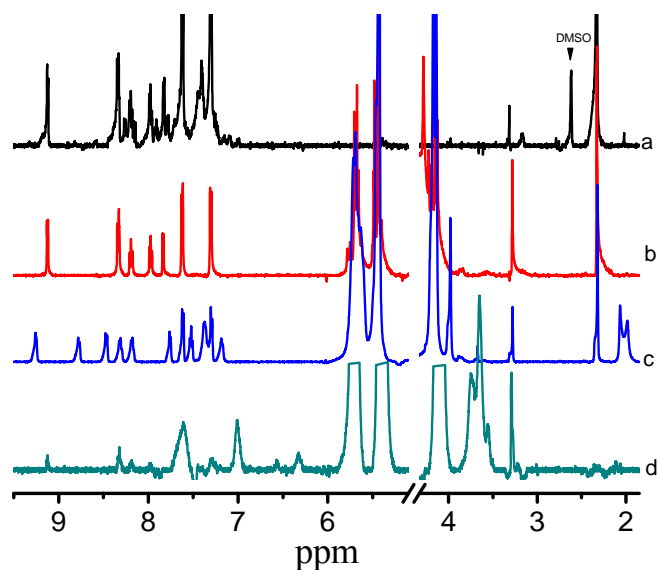


Fig. S3. ¹H NMR spectra of TO in D₂O before and after addition of 2 equiv of CBs at 25°C (a: TO; b: TO+CB[6]; c: TO+CB[7]; d: TO+CB[8]).

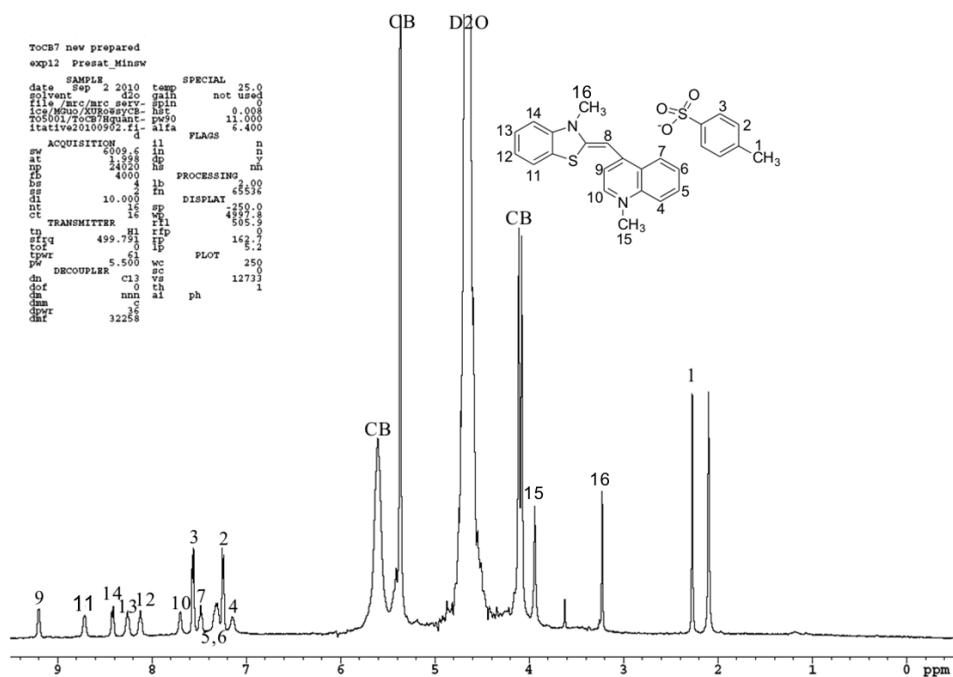


Fig S4. ¹H NMR spectrum of CB[7]/TO inclusion complex in D₂O.

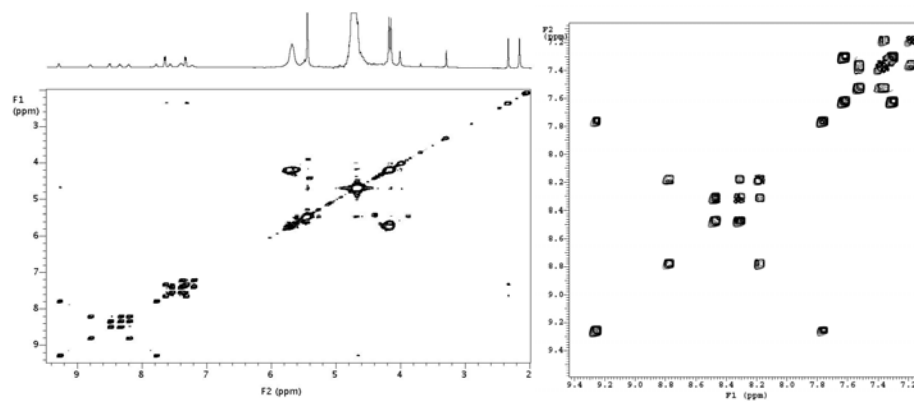
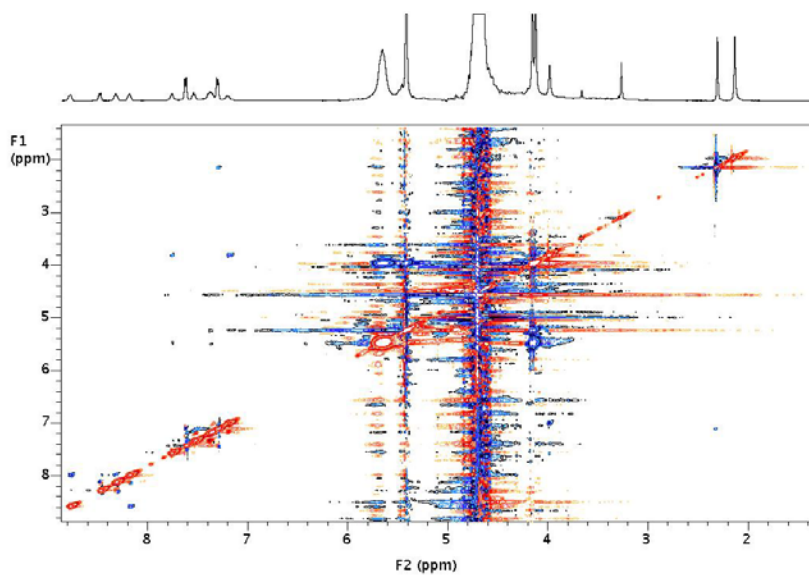


Fig S5. COSY 2D spectrum of CB[7]/TO inclusion complex in D₂O.



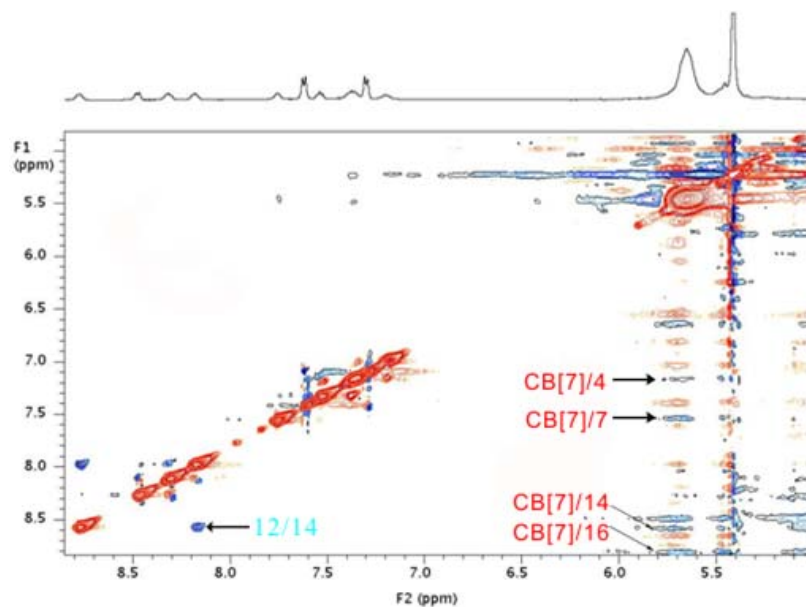


Fig S6. Rotating frame NOE (ROESY) spectra of CB[7]/TO inclusion complex in D_2O .

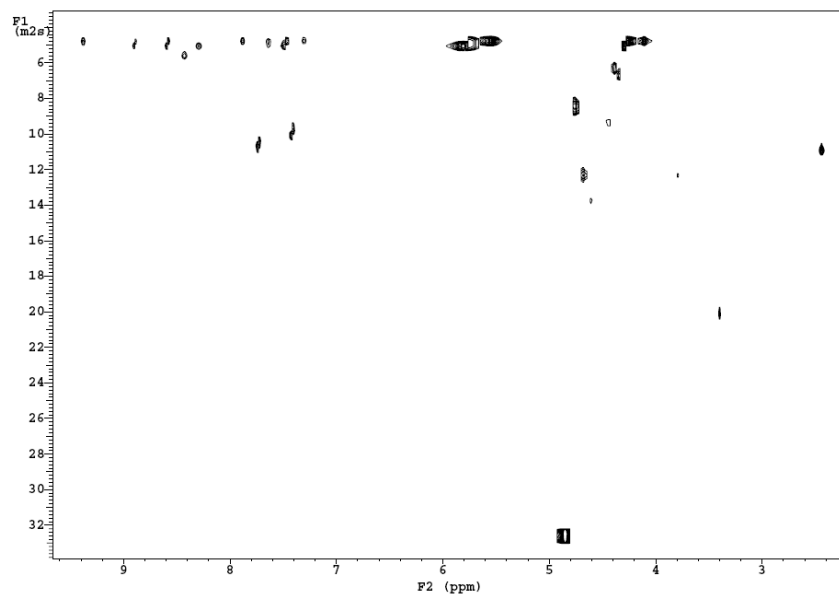


Fig S7. Diffusion-ordered 2D NMR (DOSY) spectrum of CB[7]/TO inclusion complex in D_2O at $25\text{ }^{\circ}C$.

Figure S7 is the Diffusion-ordered 2D NMR spectrum, DOSY of TO in D_2O at $25\text{ }^{\circ}C$. Although TO is a single molecule, two kinds of diffusion constants can be unambiguously extracted from the DOSY spectrum that is diffusion constant of TO core of $7.81 \times 10^{-10}\text{ m}^2/\text{s}$ and the counter ion of $12.13 \times 10^{-10}\text{ m}^2/\text{s}$. Figure S5 shows the 2D DOSY spectrum of TO and CB[7] complex in D_2O at $25\text{ }^{\circ}C$. The spectrum

indicated that after putting the CB[7] to the TO aqueous solution, the diffusion constant of guest TO decrease to the same value of the host CB[7]. That is $4.97 \times 10^{-10} \text{ m}^2/\text{s}$. The same diffusion constant of the host and guest is the strong indication of the formation of inclusion complex. While the positive charged core of the guest TO is included inside of the host CB[7], the anion counter ion is in the vicinity of the inclusion complex. Although the diffusion constant, $10.79 \times 10^{-10} \text{ m}^2/\text{s}$ of the counter ion is larger than the inclusion complex, it is smaller compare to the free guest. The solubility of the TO in water increase dramatically after add CB[7]. This is the evidence of the strong inclusion complex formed which is consistent with the fluorescence kinetic result. The DOSY NMR data also shows that there is no free TO signal detected in the aqueous solution of the complex system although there are extra TO solid in the bottom of the NMR tube. The result indicates that the inclusion complex is very strong which is consistent with the fluorescence kinetic result.

The hydrodynamic volume of the complex was estimated by the ratio $V_{\text{complex}}/V_{\text{CB[7]}}$, where V_{complex} and $V_{\text{CB[7]}}$ represent the volumes of the complex and CB[7], respectively, which was calculated from the diffusion coefficient ratio ($V_{\text{complex}}/V_{\text{CB[7]}} = (D_{\text{complex}}/D_{\text{CB[7]}})^{-3}$).^{S4} The ratio of the hydrodynamic volume of TO/CB[7] and TO measured by the DOSY NMR technique is 3.88.

S4. Ko, Y. H.; Kim, K.; Kang, J.-K.; Chun, H.; Lee, J. W.; Sakamoto, S.; Yamaguchi, K.; Fettinger, J. C.; Kim, K. *J. Am. Chem. Soc.* **2004**, *126*, 1932-1933.

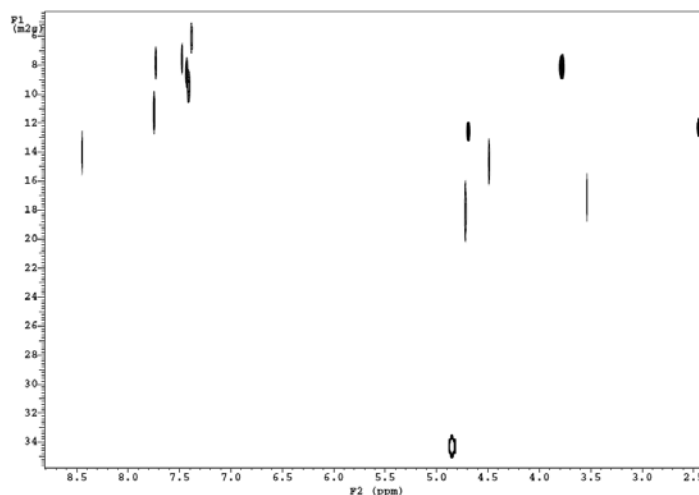


Fig S8. DOSY spectrum of CB[8]/TO inclusion complex in D₂O at 25 °C.

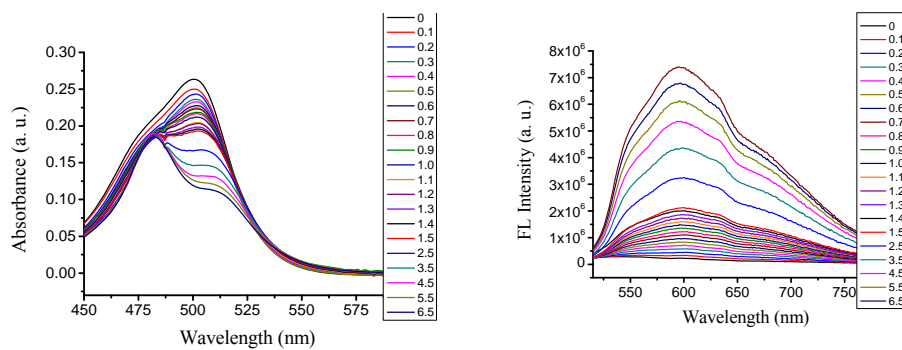


Fig S9. Absorption (a) and fluorescence (b) change of Thiazole Orange (5 μM) in aqueous solution upon addition of CB[7].

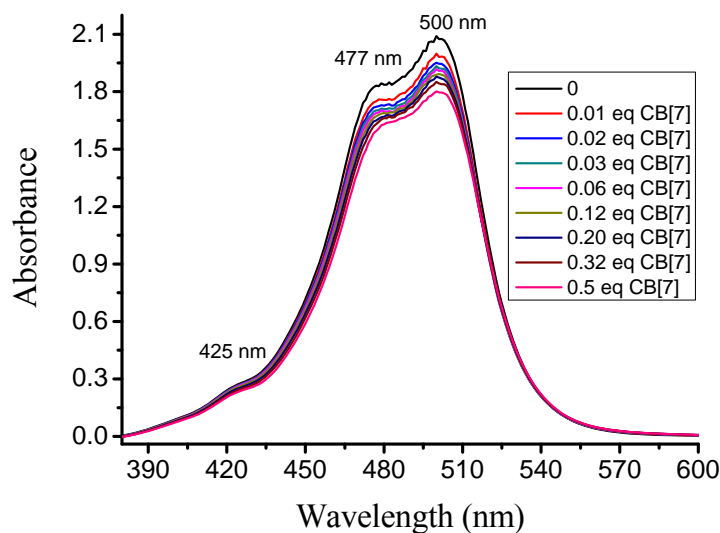


Fig S10. Absorption change of Thiazole Orange (50 μM) in aqueous solution upon addition of CB[7].

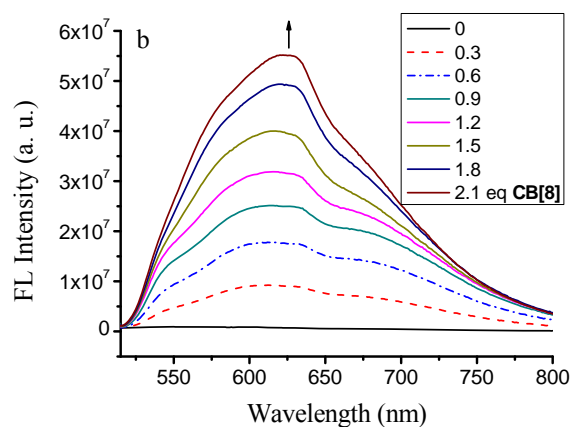


Fig. S11 Fluorescence change of Thiazole Orange (TO) (5 μ M) in aqueous solution upon addition of CB[8].

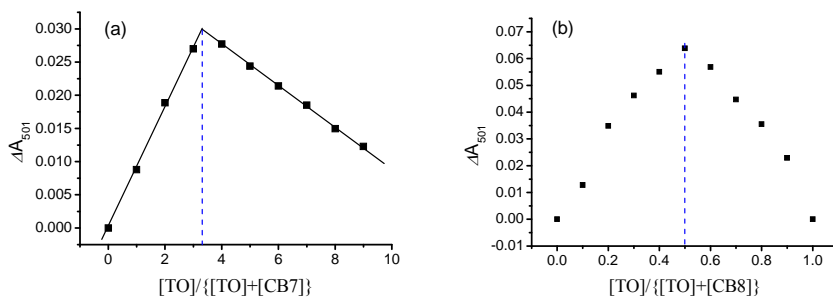


Fig S12. Figure. Job plot for the complexation of TO with CB[7] (a) and CB[8] (b) in water.

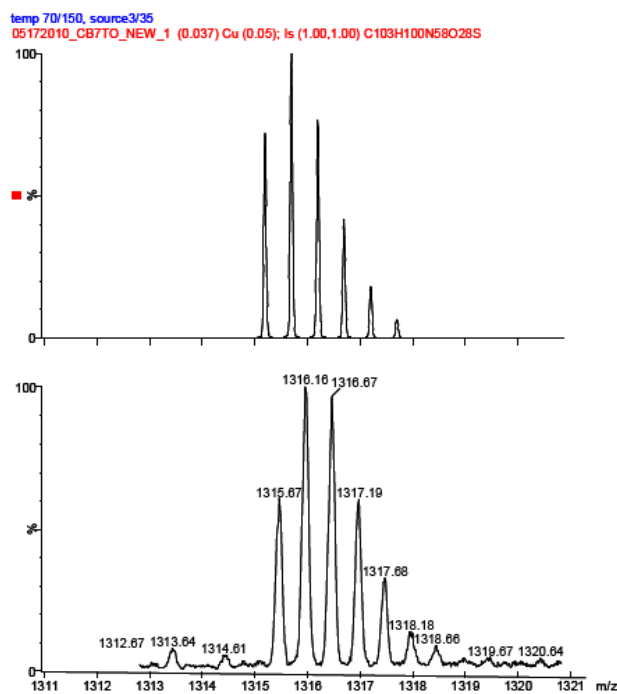


Fig S13. Mass spectra of TO:CB[7] (1:2) complex. The experimental isotopic pattern of TO·(CB[7]₂) complex (bottom spectrum) matches the theoretical prediction (top spectrum) for TO·(CB[7]₂) (without counter ion).

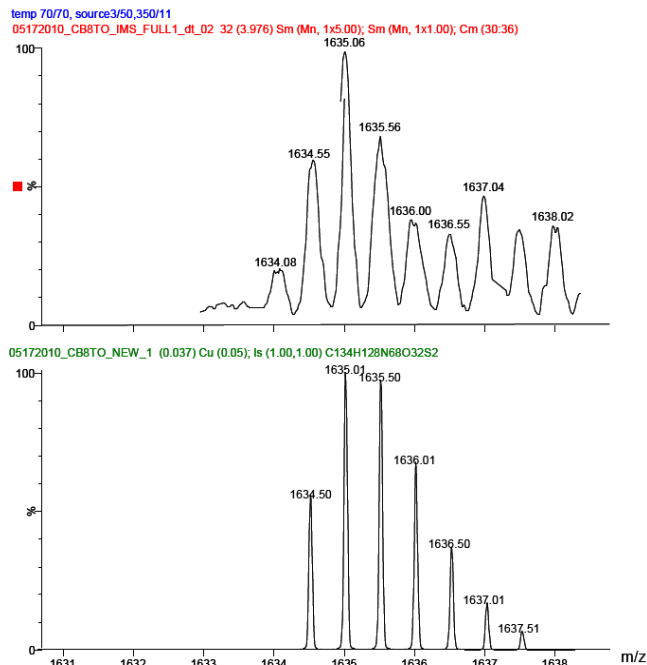


Fig S14. Mass spectra of TO₂:CB[8] (2:2) complex. The experimental isotope pattern of TO₂·(CB[8])₂ complex (top spectrum) matches the theoretical prediction (bottom spectrum) for TO₂·(CB[8])₂(without counter ion).

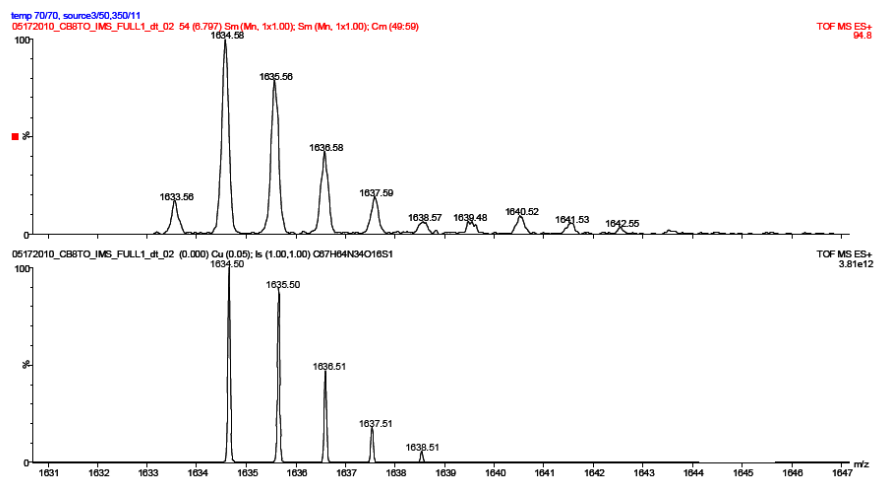


Fig S15. Mass spectra of TO:CB[8] (1:1) complex. The experimental isotope pattern of TO·CB[8] complex (top spectrum) matches the theoretical prediction (bottom spectrum) for TO·CB[8] (without counter ion).

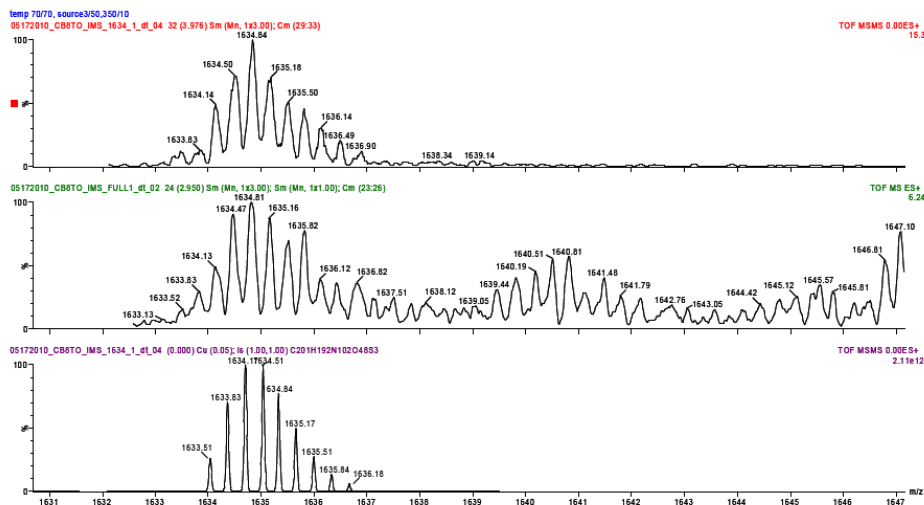


Fig S16. Mass spectra of TO:CB[8] (3:3) complex. The experimental isotope pattern of $\text{TO}_3 \cdot (\text{CB}[8])_3$ complex (top two spectra) matches the theoretical prediction (bottom spectrum) for $\text{TO}_3 \cdot (\text{CB}[8])_3$ (without counter ion).

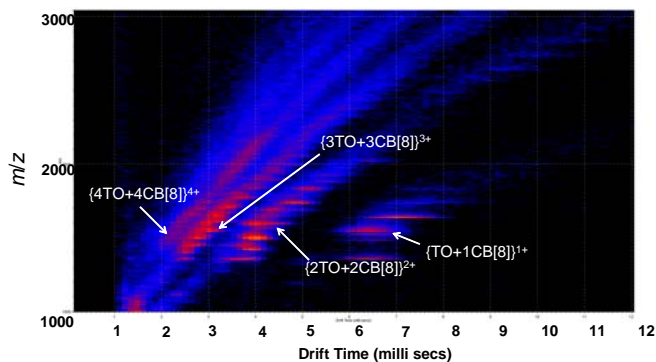


Figure S17, Two-dimensional ESI-TWIM-MS plot for m/z 1634. Complexes analyzed on the Waters Synapt quadrupole/time-of-flight (Q/ToF) mass spectrometer at a traveling wave height of 9.3 V and velocity of 380 m/s. Ion mobility separation gave signals at different time (ms), corresponding to linear $\text{TO}_4 \cdot (\text{CB}[8])_4$, $\text{TO}_3 \cdot (\text{CB}[8])_3$, $\text{TO}_2 \cdot (\text{CB}[8])_2$ and $\text{TO} \cdot \text{CB}[8]$, respectively.

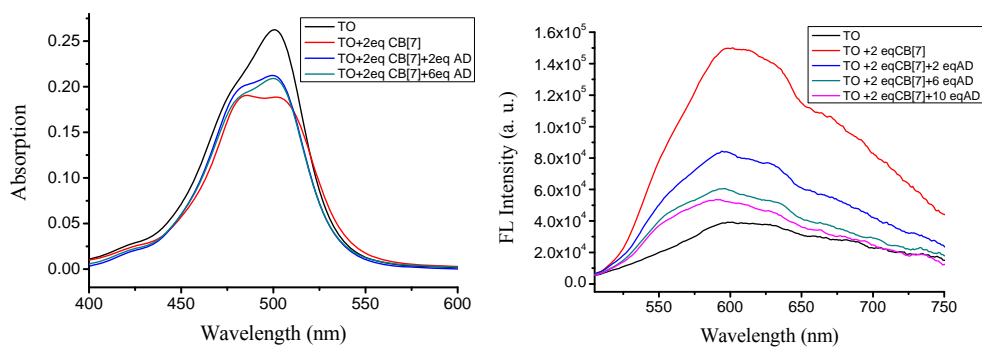


Fig S18. Absorption and fluorescence change of TO (5 μ M) in water with AD in the presence of 2 equiv of CB[7].

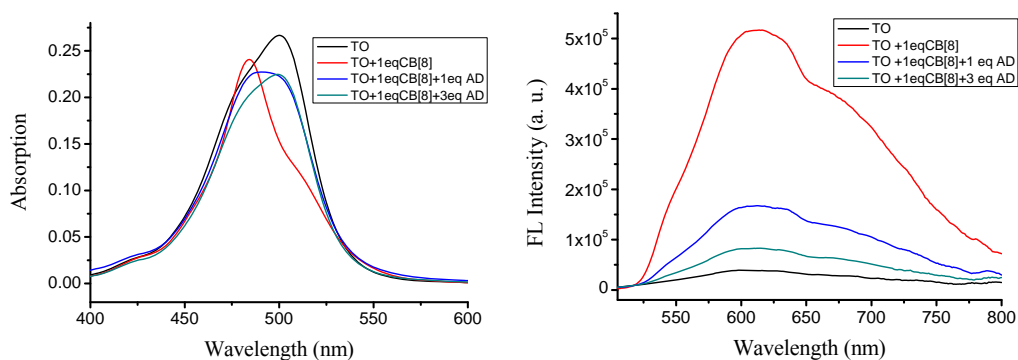


Fig S19. Absorption and fluorescence change of TO (5 μ M) in water with AD in the presence of 1 equiv of CB[8].

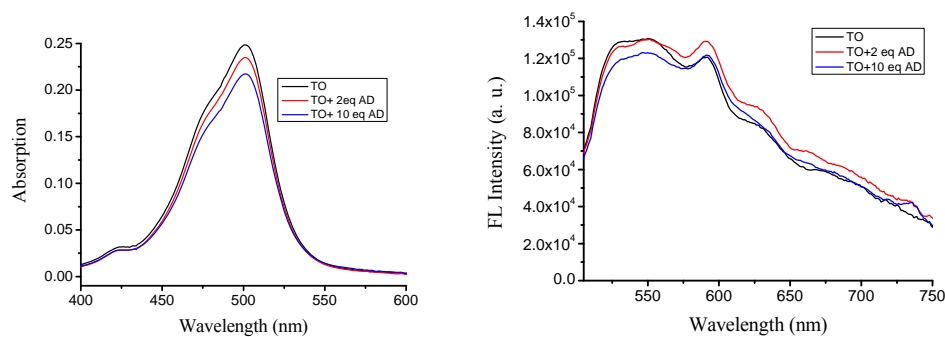


Fig S20. Absorption and fluorescence change of TO (5 μ M) in water with AD in the absence of CBs.

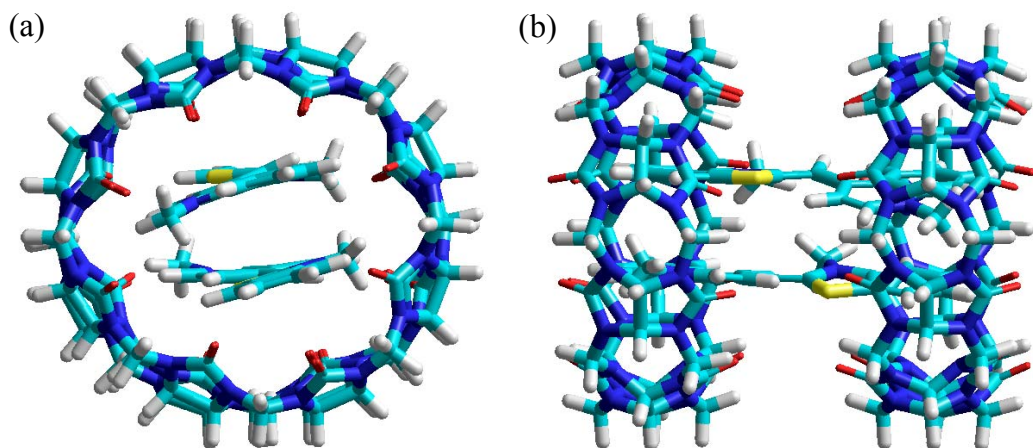


Fig. S21. Optimized structure of 2TO + 2CB[8] (by using HyperChem AM1 setting) in front (a) and side (b) view.

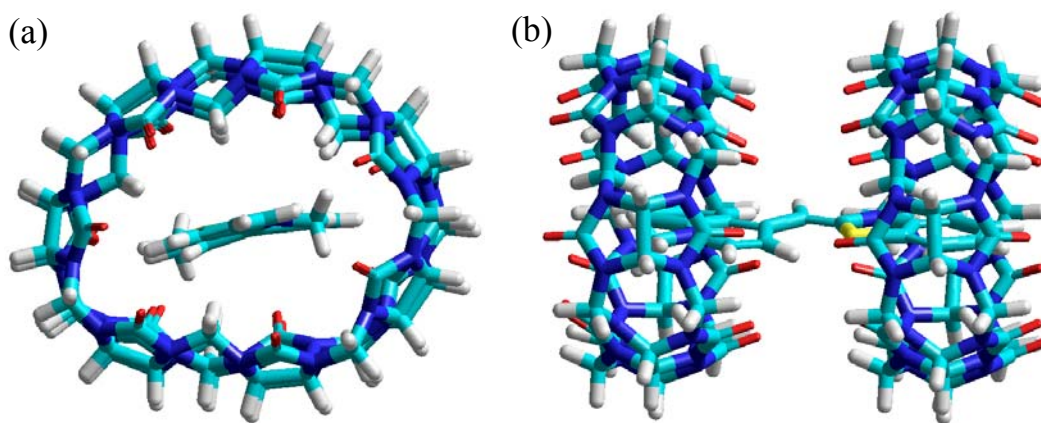


Fig. S22. Optimized structure of TO + 2CB[7] (by using HyperChem AM1 setting) in front (a) and side (b) view.

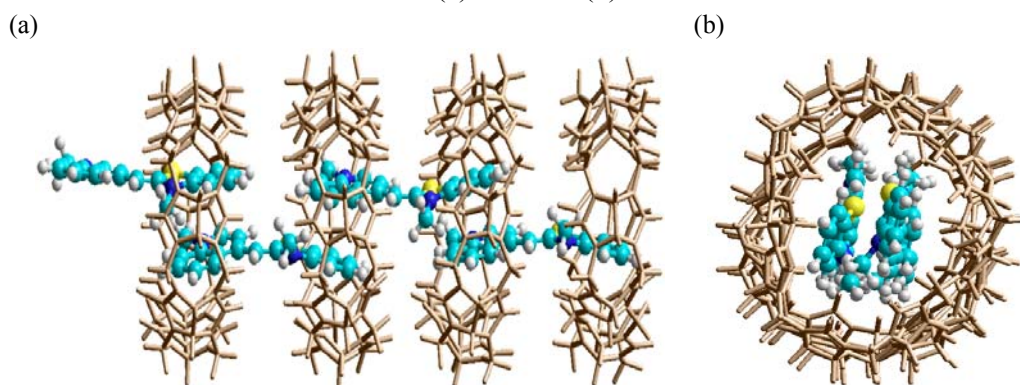


Figure S23. Molecular modeling of “TO+CB[8]” oligomer in front (a) and side (b) view. The geometry was optimized by using HyperChem (using Molecular Mechanics Force Field MM+). For clarity, the CB[8] is constructed with stick model and shown in brown color.

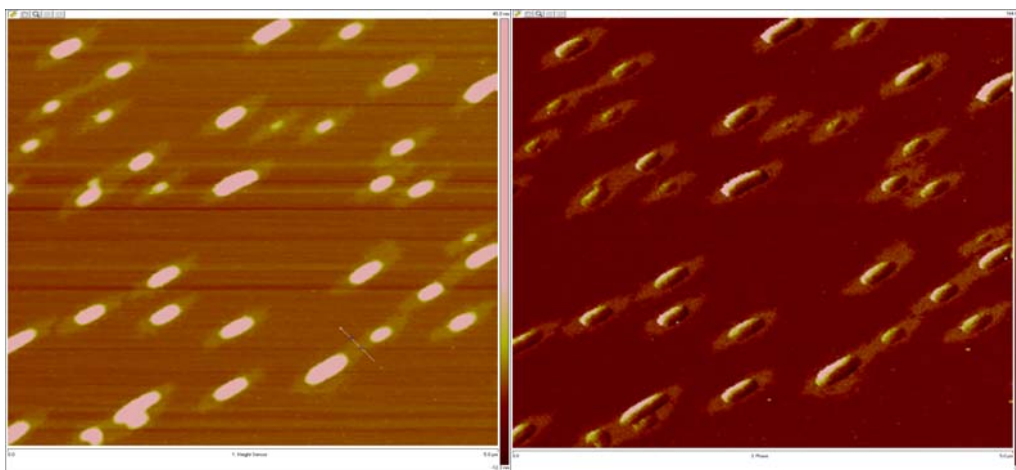
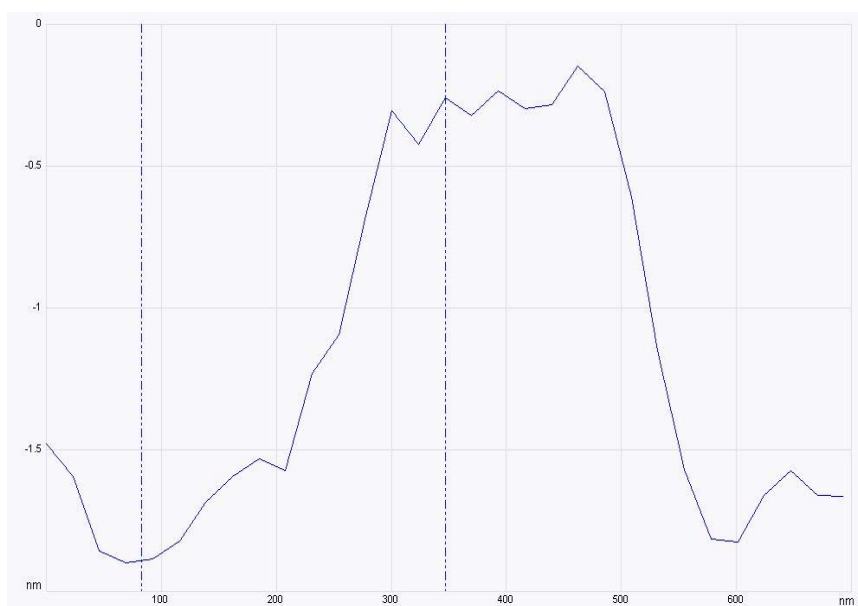
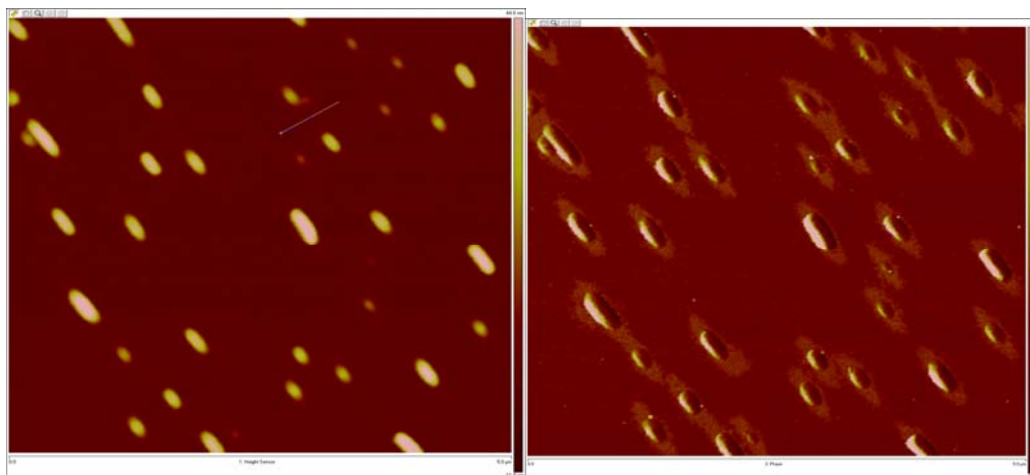




Fig. S24. AFM images and cross section profiles of TO and CB[7] spin-coated on the mica surface. (the height is about 1.4-1.6 nm, which is consistent with the size of CB[7] (CB[7] is 1.6 nm).

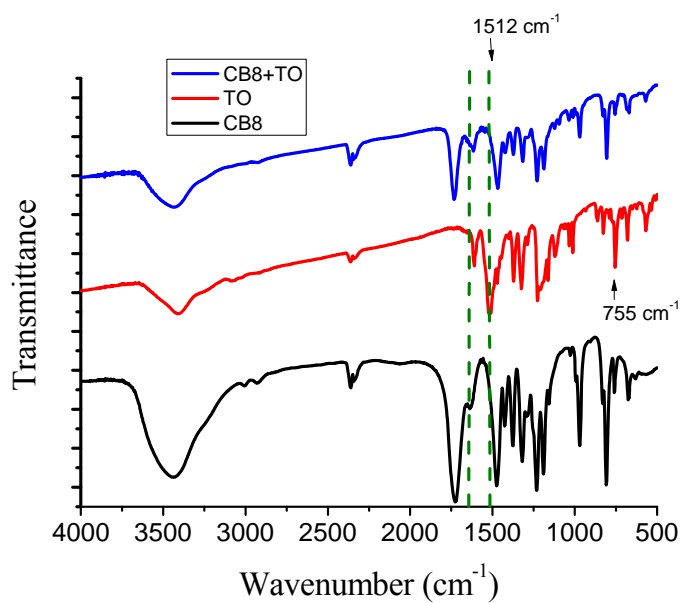


Fig. S25. IR spectrum of TO, TO+CB[8] and CB[8]. The strong band at 1735 cm⁻¹ was attributed to C=O. The band at 755 cm⁻¹ was assigned to quaternary amine salt.